JOURNAL OF GUIDANCE, CONTROL, AND DYNAMICS
Vol. 15, No. 2, March-April 1992

Engineering Notes

ENGINEERING NOTES are short manuscripts describing new developments or important results of a preliminary nature. These Notes cannot exceed 6 manuscript pages and 3 figures; a page of text may be substituted for a figure and vice versa. After informal review by the editors, they may be published within a few months of the date of receipt. Style requirements are the same as for regular contributions (see inside back cover).

Smooth Blend of Time-Optimal and Linear Control

C. A. Harvey*
University of Minnesota, Minneapolis, Minnesota 55455
and
D. J. Bugajski†
Honeywell, Inc., Minneapolis, Minnesota 55418

Introduction

OPTIMAL control of systems with saturating control has a long history of development.[1] Here, in a slightly different approach, a smooth blend of time-optional control with a given linear control is developed. We are motivated by acquisition, pointing, and tracking applications, where linear pointing and tracking controllers with sufficient low frequency gain to provide accurate pointing and with enough integrators to provide adequate tracking encounter significant performance degradation because of actuator saturation. Blending time-optimal and linear control can alleviate these problems, but discontinuities in the control signal or its derivatives can excite flexure modes. Thus, smooth transitions between linear and nonlinear control as well as smooth switches in the controller are desired. A design model for the system considered is a single-input/single-output, rigid-body approximation of a fairly stiff structure for which highly accurate linear regulation of small errors and rapid reduction of large initial errors are desired. Commands to this system may be polynomials in time representing target motion to be tracked. The major contributions of the Note are methods for initializing the linear controller at boundaries of the linear region and for smooth transitions between extremes in a feedback form to replace bang-bang switching.

Control Law Derivation

A single-loop system is shown in Fig. 1, with the rotational dynamics of the plant modeled as an inertia and a saturating torque. A model of the torque limit is incorporated in the control law so that the limiter in the loop is redundant, except that the actual torque limit T_L may differ from the limit in the model. The torque limit in the model t_L is assumed to be equal to T_L in this derivation. The transfer function of the linear controller $u_L(t)$ is assumed to be

$$U_L(s)/E(s) = K(s)^*[V(s)/E(s)] \tag{1}$$

where $E(s)$ is the Laplace transform of the error signal $e(t)$ and

$$V(s)/E(s) = k_1 s + k_2 \tag{2}$$

Thus, $v(t)$ may be viewed as a proportional-plus-derivative controller, and $K(s)$ consists of additional compensation for high-frequency attenuation and low-frequency integration. We assume that $|K(j\omega_c)| \approx 1$, where ω_c is the crossover frequency of the linear system if $v(t)$ is used as the control with k_1 chosen to give good damping and k_2 chosen to give the desired bandwidth. Of course, the chosen bandwidth must be consistent with the fidelity of the design model.

The phase plane (e vs $\dot{e}$) is convenient for analysis of the system with bang-bang control or with proportional-plus-derivative control. The linear region for a combination of v control and time-optimal control should be a subset of the linear strip in the phase plane where the magnitude of $v(t)$ is less than T_L. If the linear region is chosen to be the section of the strip with $|\dot{e}| \leq \alpha$, then the switching curves for time-optimal control to this linear region consists of parabolic arcs passing through the upper left-hand and lower right-hand vertices of the linear region.[2] But for simplicity in blending the linear and nonlinear controls, we will take the switching curves to be the parabolic arcs passing through the upper right-hand and lower left-hand vertices of the linear region. An example of such a linear region R_1 and the associated switching curves are shown in Fig. 2, with α chosen so that the parabolas defining the switching curves pass through the origin. Taking the control to be $u_L(t)$ inside R_1 and to be bang-bang outside of R_1 as the basis for blended control, it remains to provide smooth transitions of the feedback controller throughout the phase plane. Smoothing must be provided across 1) the switching curves and 2) the boundaries of R_1.

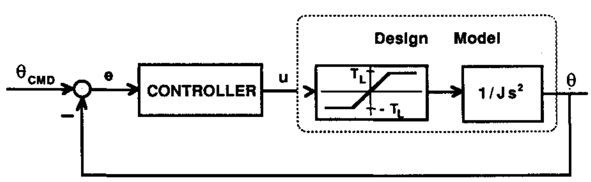

Fig. 1 Block diagram of single-loop system.

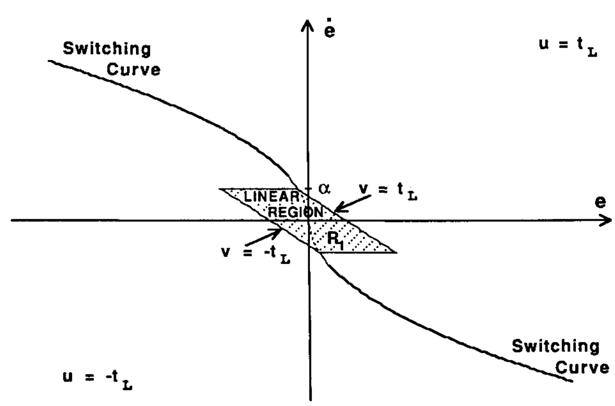

Fig. 2 Typical switching curves and linear region.

Received May 7, 1990; presented as Paper 90-3422 at the AIAA Guidance, Navigation, and Control Conference, Portland, OR, Aug. 20-22, 1990; revision received Oct. 9, 1990; accepted for publication Oct. 22, 1990. Copyright © 1991 by the American Institute of Aeronautics and Astronautics, Inc. All rights reserved.

*Professor, Aerospace Engineering and Mechanics; currently, Visiting Professor, Department of Electrical Engineering, National University of Singapore, 10 Kent Ridge Crescent, Singapore 0511, Republic of Singapore. Member AIAA.

†Research Engineer, Systems and Research Center, 3660 Technology Drive.

Smoothing Across Switching Curves

To remove discontinuities in the control at the switching curves, a transition region can be defined as follows. Suppose that the nonlinear control is constrained so that transitions from t_L to $-t_L$ (or from $-t_L$ to t_L) must occur along cosine profiles in a time interval of $1/(2N)$ s. Such a transition is

$$u(t) = t_L \cos[2N\pi(t-t_0)] \quad \text{for } t_0 < t < t_0 + [1/(2N)] \qquad (3)$$

Then, ignoring a terminal discontinuity, there would be transition regions: R_2 between the curves C_1 and C_2 and R_3 between the curves C_3 and C_4 as shown in Fig. 3 where (defining $U = t_L/J$):

C_1:

$$e_1 = [-\dot{e}^2/(2U)] - [\dot{e}/(2N)] - [2U/(2N\pi)^2] \quad \text{for } \dot{e} > 0 \qquad (4)$$

C_2:

$$e_2 = -\dot{e}^2/(2U) \quad \text{for } \dot{e} > 0 \qquad (5)$$

C_3:

$$e_3 = [\dot{e}^2/(2U)] - [\dot{e}/(2N)] + [2U/(2N\pi)^2] \quad \text{for } \dot{e} < 0 \qquad (6)$$

C_4:

$$e_4 = \dot{e}^2/(2U) \quad \text{for } \dot{e} < 0 \qquad (7)$$

The curves C_2 and C_4 are trajectories corresponding to $u = |t_L|$, and C_1 and C_3 are easily determined from the equations of motion using a transition control in the form of Eq. (3) with termination of the transition on C_2 and C_4. In Fig. 3, N is selected for simplicity such that the transition curves intersect R_1 at its vertices. Other cases are slightly more complicated.

Implementing the cosine profiles exactly in a feedback law requires solving a pair of nonlinear equations, whereas a good approximation is provided by setting

$$u = t_L \cos(\pi\lambda) \qquad (8)$$

where

$$\lambda(e,\dot{e}) = [e - e_2(\dot{e})]/[e_1(\dot{e}) - e_2(\dot{e})] \quad \text{if } \dot{e} < 0$$

$$= [e - e_3(\dot{e})]/[e_4(\dot{e}) - e_3(\dot{e})] \quad \text{if } \dot{e} > 0 \qquad (9)$$

where $e_j(\dot{e})$ is defined by Eqs. (4–7). With Eq. (8) as the control law for the transition region, the nonlinear portion of the controller has the desired smoothness between the regions R_4 and R_5 where $u = |t_L|$ (see Fig. 3). With this approximation, it can be shown that complete transitions from $-t_L$ to t_L or from t_L to $-t_L$ will not take place, so that if a trajectory enters the region R_2 or R_3, then it remains in the interior of that region until it reaches R_1.

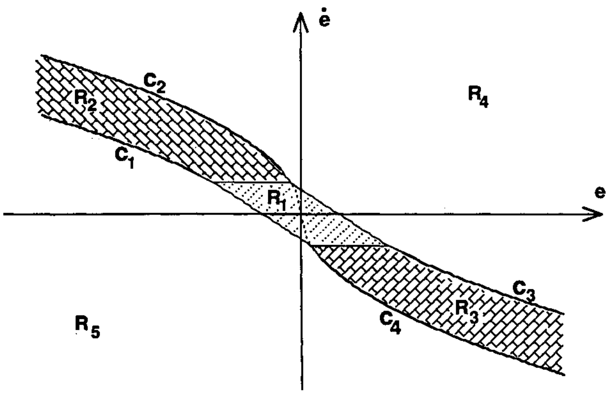

Fig. 3 Transition curves and control mode region.

Smoothing Nonlinear/Linear Transitions

The following initialization procedure may be used to obtain smooth transitions between linear and nonlinear control. Let the state-space representation of $K(s)$ in Eq. (1) be

$$\dot{e} = A_x + B_v, \qquad u_L = Cx \qquad (10)$$

where v is given by Eq. (2) or in the time domain as $v = k_1(\dot{e}) + k_2 e$ each time R_1 is entered, and an initial value x_0 is to be determined. Expressions for u_L and its derivatives in terms of x, v, and derivatives of v can be obtained by differentiating Eq. (10). For example,

$$u_L = Cx, \qquad \dot{u}_L = CAx + CBv$$

$$\ddot{u}_L = CAx + CABv + CB\dot{v}, \qquad \text{etc.} \qquad (11)$$

At an entry to R_1, the values of e, $\dot{e}$, v, and u and its derivatives are known. But continuity conditions for second and higher order derivatives of u involve derivatives of v, which are not known. To obtain estimates, let v^* denote "ideal values" of v and its derivatives, where we assume ideal motion emanates from the boundary of R_1 according to the ideal system:

$$\frac{\mathrm{d}}{\mathrm{d}t}[e\dot{e}]' = A_e [e\dot{e}]' \qquad (12)$$

$$v^* = C_e [e\dot{e}]' = [k_2 k_1][e\dot{e}]' \qquad (13)$$

where A_e can be chosen to provide desired behavior near the boundary of R_1. Replacing the derivatives of v with those of v^* [computed from Eqs. (12) and (13)] in Eq. (11) yields

$$Cx_0 = u, \qquad CAx_0 = \dot{u} - CBv$$

$$CA^2x_0 = \ddot{u} - CABv - CB\dot{v}^*, \qquad \text{etc.} \qquad (14)$$

which may be solved for x_0. These initial conditions will provide smooth control transitions with possible discontinuities in the second derivative.

Smoothing Startup and Exits from the Linear Region

The only remaining possibilities for discontinuous control are at startup and at exits from R_1. A programmed cosine profile may be used to provide a smooth startup. In this case, for $0 \le t \le t_0$, the control command is computed as described earlier and then multiplied by the sinusoid, $[1 - \cos(\pi t/t_0)]/2$. This same procedure can be used for exits from R_1, where the clock for the sinusoid is started at the exit time and the difference between the computed control and the exit control is multiplied by the sinusoid and added to the exit control. The value of t_0 can be chosen to be consistent with the choice of N.

Design Parameters

In the definition of the control law, there are four parameters to be chosen by the designer: N, t_L, the height of R_1, and the bandwidth of the linear system. Changing the height of R_1 without significantly increasing the complexity of the control law can be accomplished by keeping the intersections of the switching and transition curves with R_1 at the same vertices of R_1. Then the parameter N is determined, and Eqs. (4–7) can be modified to account for the translations of the vertices along the slanted lines defined by $|v| = t_L$. The torque limit in the model t_L is also a design parameter that has the effect of scaling R_1. Finally, changing the bandwidth of the linear system changes the slopes of the slanted sides of R_1.

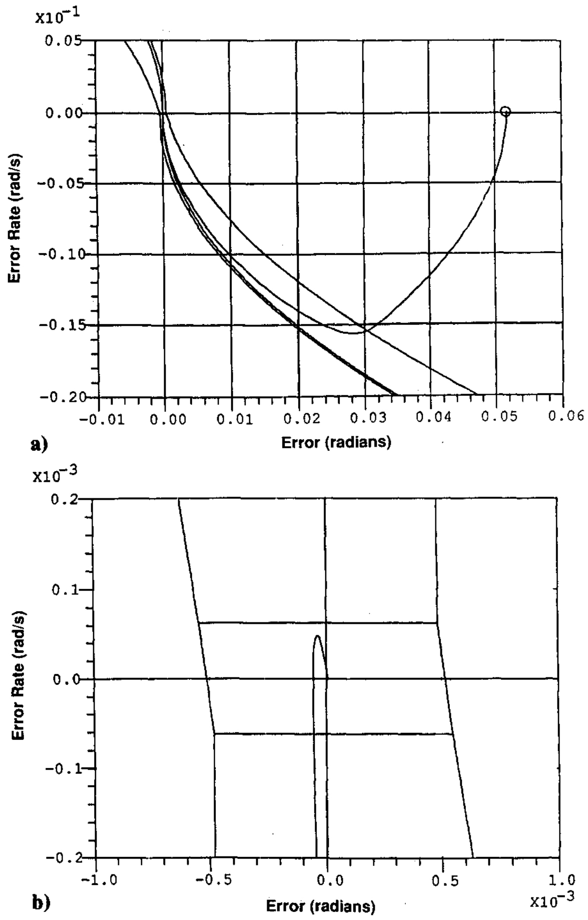

Fig. 4 Example of error trajectory in the phase plane.

Example

Simulation analysis played a key role in the development of this control law, being critical for quantitive evaluation of control system performance as a function of design parameters for any specific application. In this example, the control system is required to null pointing errors while tracking a target whose motion is given by

$$\theta_{CMD}(t) = \theta_p + \theta_v(t) + \theta_a(t^2/2) + \theta_j(t^3/6) \tag{15}$$

where θ_p, θ_v, θ_a, and θ_j are randomly chosen within prescribed bounds. To meet the tracking requirement, the linear control law needed two integrators. A second-order, high-frequency attenuation was included in the linear controller. Thus, $K(s)$ in Eq. (1) was selected as

$$K(s) = k(s^2 + as + b)/[s^2(s^2 + cs + d)] \tag{16}$$

The values of the parameters of the design model for this example are $J = 70$ kgm^2 and $T_L = 0.4$ Nm. The design parameters chosen for the control law are 1) $t_L = T_L$, 2) the linear control bandwidth = 8 rad/s, and, finally, 3) the height of R_1 is 1/20th of that shown in Fig. 3, and the switching and transition curves are chosen to pass through the vertices of R_1.

The performance of the control law is demonstrated via simulation of a sample target trajectory. The error trajectory in the phase plane for this case is shown in Fig. 4a, and Fig. 4b shows an enlargement of the phase plane near R_1. In both parts, the switching and transition curves are shown, and in Fig. 4a the switching curve for time-optimal control to the origin is also shown. Figure 5 shows the profile of the control torque. It consists of a continuous startup, a single period of saturation, a transition segment, and at about 5 s, a smooth change from the transition control to the linear control law.

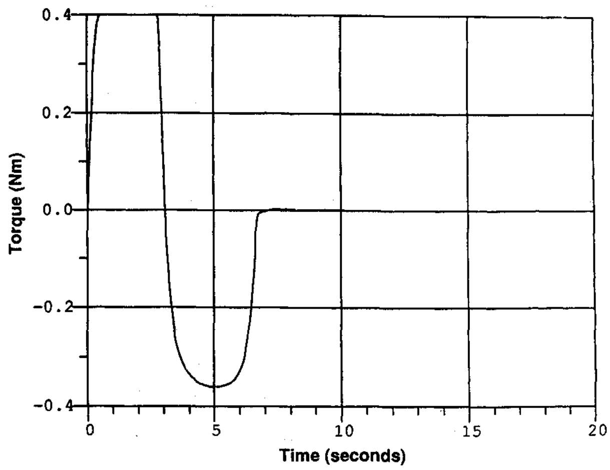

Fig. 5 Example of torque profile.

Conclusions

A blend of linear and time-optimal control is capable of providing acquisition, tracking, and pointing with high accuracy and short response times. Smoothness in a blended feedback control law can be obtained for low-order design models, and simulation is a necessary ingredient in the derivation of such a controller.

References

[1]Oldenburger, R., *Optimal and Self-Optimizing Control,* M.I.T. Press, Cambridge, MA, 1966.

[2]Harvey, C. A., "Synthesis of Time-Optimal Control for Linear Processes," *Journal of Mathematical Analysis and Applications,* Vol. 10, 1965, pp. 334–341.

Projective Formulation of Maggi's Method for Nonholonomic Systems Analysis

Wojciech Blajer*
Technical University of Radom,
26-600 Radom, Poland

Introduction

THOUGH first published late in the last century, Maggi's equations, until quite recently, have not been applicable in practice and primarily have been of academic interest only.[1] In a recent paper,[2] however, Papastavridis shows a variety of practical implementations of Maggi's approach as an efficient technique for the dynamic analysis of systems subject to nonholonomic constraints. In this Note, a geometrical insight into Maggi's method is presented. Based on the concept of the projection method,[3] the present formulation consists of the partition of the system's configuration space into the orthogonal and tangent subspaces; the orthogonal subspace is spanned by the constraint vectors, and the tangent subspace complements the orthogonal subspace in the configuration space. The projection of the initial (multiplier-containing) dynamical equations into the tangent subspace gives the con-

Received July 2, 1990; revision received Nov. 1, 1990; accepted for publication Nov. 16, 1990. Copyright © 1991 by the American Institute of Aeronautics and Astronautics, Inc. All rights reserved.

*Lecturer, Department of Mechanics, ul.Malczewskiego 29; currently Research Fellow, University of Stuttgart, Institute B of Mechanics, D-7000 Stuttgart 80, Germany.